

UDC 538.971

RELAXATION MECHANISM OF NONPOLAR $(1\bar{1}00)$ AND $(11\bar{2}0)$ SURFACES OF ZINC OXIDE: AB INITIO CALCULATIONS

A.B. Usseinov, A.T. Akilbekov, A.K. Dauletbekova

L.N. Gumilyov Eurasian National University, Mirzoyana str. 2, 010008, Astana,
useinov_85@mail.ru

This paper presents ab initio calculations of non polar $(1\bar{1}00)$ and $(11\bar{2}0)$ surfaces of zinc oxide. It is shown that the $(11\bar{2}0)$ surface more stable than the $(1\bar{1}00)$ surface. Electronic relaxation causes redistribution of charge across the surface, where a considerable covalent contribution to chemical bonding is observed. Analysis of vertical ionic displacements showed a typical relaxation picture: after slab relaxation the surface Zn ions are displaced inwards to the slab center, whereas O ions are slightly shifted in the same direction, thus, the anions lies above the cations that usually observed for metal-oxide surfaces.

Key words: ab initio calculations, ZnO surface, surface energy.

Introduction

Zinc oxide (ZnO) has received great attention being widely used for producing optoelectronic devices and transparent conductive thin films [1]. Due unique atomic and electronic structure, ZnO is a prospective material for producing LED displays, transparent conductive thin films, laser and UV light-emitting diodes [2-6].

Beside the structural and electronic properties of ZnO bulk, the investigation of ZnO surfaces also attracted significant attention in recent years due a wide variety of applications such as catalysis and most recently nanomaterials [7]. As is known, various ZnO surfaces are widely used as catalyst for methanol synthesis chemical reaction [8]. Note that catalytic properties of ZnO surfaces improving when interacting with Cu particles. Its ability to actively react with hydrogen enables using it as a hydrogen accumulating system (hydrogen power engineering), in hydrogenation and dehydrogenation processes and for making proton-exchanged membranes for fuel cells [9]. Application range of various ZnO surfaces is increasing with the new technologies of producing thin ZnO films with different nanostructures [10]. Despite to wide practical applications of different physical and chemical properties of ZnO surfaces, the atomistic picture of interaction between various adsorbents with ZnO surfaces remains a controversial issue and is being actively discussed [10].

Under normal conditions, ZnO has a wurtzite structure (B4) with hexagonal atomic Zn and O planes stacked alternately along the c – axis within the crystal lattice. In such a structure, Zn atoms have four bonds with O atoms along the c – axis and vice versa. Surface atomic structure can be characterized by four low-index surfaces: nonpolar $(10\bar{1}0)$, $(11\bar{2}0)$ surfaces and polar $(000\bar{1})$ -Zn, $(000\bar{1})$ -O surfaces. By ion sputtering and annealing at not too high temperatures all four ZnO surfaces can be prepared [7, 10]. Unlike its bulk atomic structure, surface Zn and O atoms have one «dangling» chemical bond, which results in redistribution of the charge across the surface. Thus, the surfaces are unstable structures and they are subject to atomic and electronic relaxation.

Unlike to the polar surfaces (not considered here), the nonpolar surfaces lack the extra electrostatic charge and are more stable in terms of energy. Earlier, the $(10\bar{1}0)$ ZnO surface has become an object of extensive experimental studies. By experimental study of this surface, Duke et al. [11] by low-energy electron diffraction (LEED) showed that Zn atoms on the surface are displaced inwards the ZnO crystal by $d(\text{Zn}) \approx -0.4 \text{ \AA}$, whereas O atoms are displaced downwards

only by $d(\text{O}) \approx -0.05 \text{ \AA}$, leading to a tilt ($\sim 12^\circ$) of Zn-O surface structure, which is typical for many oxide materials. The strong inward relaxation of the Zn ion was later confirmed by Gopel et al. [12] in an angle-resolved photoemission experiment. However, recent *ab initio* hybrid calculations (using B3LYP functional) employing a basis set of Gaussian type functions shows small surface relaxation (tilt changes only $\sim 2^\circ$ – 5°) [13]. Recently, similar calculations, based on plane waves basis set [14], given larger tilt relaxation ($\sim 11.7^\circ$).

Ab initio calculations of surface energy of nonpolar ($11\bar{2}0$) surface showed similar relaxation behavior as for the nonpolar ($10\bar{1}0$) surface. The surface energy calculations indicate that it is even more unstable than polar surfaces [15]. This has been further confirmed by experimental observations: images made by scanning tunneling microscopy revealed many flat and large atomic terraces ($\sim 200 - 500 \text{ \AA}$) and deep ($\sim 35 - 50 \text{ \AA}$) trenches [16]. However, we should note that quantitative experimental data on atomic relaxation along the surface are still unknown. Similarly as for the ($10\bar{1}0$) surface, one of the theoretical tight-binding model showed that Zn atoms on the surface are vertically displaced inward the crystal by $d(\text{Zn}) \approx -0.54 \text{ \AA}$ [17], whereas by second tight-binding model has been found an almost bulk-like surface geometry [18].

Before detailed investigation of interactions between various adsorbents on the ZnO surfaces, a thorough understanding of the underlying clean ZnO surfaces is necessary.

In this paper we present *ab initio* calculations of atomic and electronic relaxation of two nonpolar ZnO surfaces: a) the ($1\bar{1}00$) surface, which has the same atomic structure as nonpolar ($10\bar{1}0$) surface and were studied earlier experimentally using the methods of ellipsometry and electronic energy loss spectroscopy [19]; b) the ($11\bar{2}0$) surface. The results of charge redistribution calculation have been analyzed in terms of Mulliken analysis, which have been accompanied by previous calculations and known experimental data. This paper is organized as follows: model and method of calculations discussed in Section 2, main results and analysis are given in Section 3, while major conclusions are presented in Section 4.

2. Model and method of calculations

Large-scale *ab initio* calculations have been performed combining the basis sets of LCAO (linear combination of atomic orbitals) method with the hybrid exchange-correlation Perdew-Burke-Ernzerhof (PBE0) functional [20] as implemented in the *CRYSTAL2009* computer code [21]. Such a hybrid functional allows us to perform very accurate calculations of the band gap, unlike the standard LDA or GGA-type functionals. The basis sets for Zn and O atoms have been taken from Ref. [22] while that for H atom from Ref. [23]. For SCF procedure, the accuracies 10^{-7} , 10^{-7} , 10^{-7} , 10^{-7} , 10^{-14} have been chosen for calculations of the Coulomb overlap, Coulomb penetration, exchange overlap, first exchange pseudo-overlap and second exchange pseudo-overlap integrals, respectively. Effective atomic charges have been estimated using the Mulliken population analysis. The integration over the Brillouin zone in the reciprocal space has been performed within a 6×6 Gilat grid.

First, we have carried out the optimization of the exponents for outermost *sp* and *d* orbitals at experimental ZnO lattice parameters in order to minimize the total energy of the bulk crystal structure. Powell method has been used to perform all optimization procedure [24]. The calculation of outer orbital exponents gave the following results, for Zn atom: $\alpha_{sp} = 0.6266813$, $\alpha_{sp} = 0.1439224$, $\alpha_d = 0.5010672$; for O atom: $\alpha_{sp} = 0.4090356$, $\alpha_{sp} = 0.1370986$.

Further, we have calculated the bulk properties of a pure ZnO supercell, which gave reliable results close to the experimental data (Table 1). The optimized lattice parameters *a* and *c* slightly overestimate those obtained in experiments ($\approx 1\%$). The error in estimate of band gap width ($\approx 3.6\%$) obtained using hybrid calculations have been found to be much smaller than the error in

standard GGA calculations (resulted in a huge underestimate of the band gap: 0.74 eV [25]). The calculated effective charges indicate considerable covalency of Zn–O chemical bonds whose population is $0.137e$.

Table 1. The optimized lattice parameters a , c and u , the effective charge q_{eff} and the band gap E_g

	PBE0	B3LYP [26]	Expt [27]
a , Å	3.26 (3.257) ^a	3.278	3.242
c , Å	5.22 (5.223)	5.287	5.187
u	0.382	–	0.382
$q_{eff}(\text{Zn, O}), e$	± 1.0	–	–
E_g , eV	3.57 (3.18)	3.38	3.44 [1]

^aResults in brackets were obtained using plane-wave approach [25]

To describe nonpolar $(1\bar{1}00)$ and $(11\bar{2}0)$ surfaces, the symmetric atomic slab model of finite thickness along the z axis and extended by (2×2) in the x and y directions has been chosen and contains odd (5, 7, 9, and 11) number of layers. Figure 1 shows the models of 5-layer atomic slabs of the reviewed nonpolar surfaces.

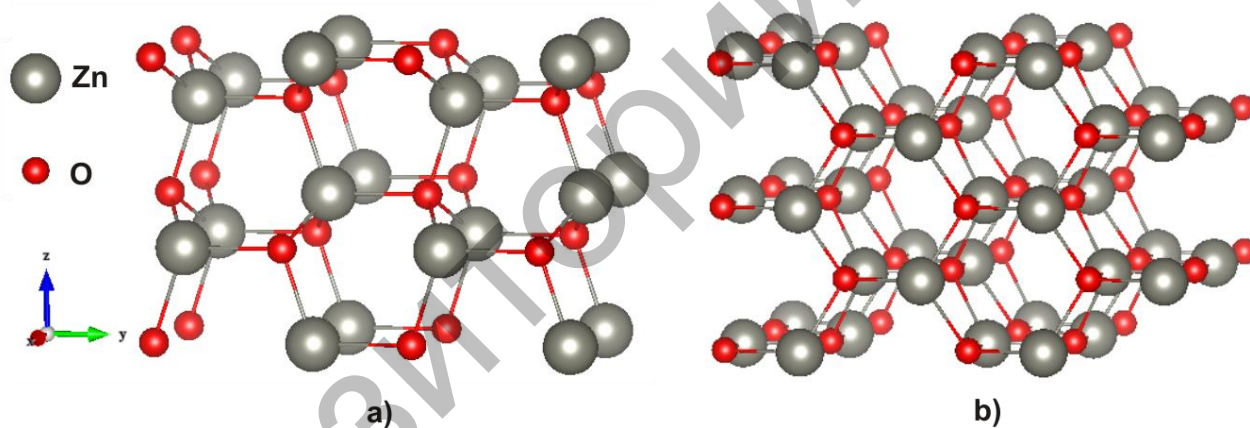


Fig.1. Models of unrelaxed 5-layer atomic slabs of the nonpolar a) $(1\bar{1}00)$ and b) $(11\bar{2}0)$ ZnO surfaces.

3. Results and analysis

First, the surface energy of nonpolar ZnO surfaces (Table 2) has been calculated as a function of a slab thickness, containing odd number (5, 7, 9, or 11) of atomic layers. Thus, we study the process of nonpolar surfaces stabilization depending on the number of layers in the slab. As shown in Table 2, the results our calculations are in line with the previous DFT hybrid calculations for nonpolar $(11\bar{2}0)$ surface. For the nonpolar $(1\bar{1}00)$ surface, the surface energy slowly reduces with increasing of the number of layers; the difference found for surface energy is 0.89 eV, suggesting that $(1\bar{1}00)$ surface is less stable than $(11\bar{2}0)$ surface [15]. Test calculations for a $(11\bar{2}0)$ surface slabs containing much more than 11 layers revealed no significant changes of the surface energy.

Also another criterion for surface stabilization is the atomic charge distribution analysis. It is not unique, but it helps compare the results and demonstrate the surface stabilization trends. Table 3 gives the results of calculations for distribution of effective atomic charges of Zn and O atoms across the first and second planes of the atomic surface slab depending on the number of

planes (layers) in the atomic slab. Distribution of effective atomic charge is obviously the same for both surfaces. For Zn and O atoms on the second atomic plane in 5-layer atomic slab with $(1\bar{1}00)$ surface, the charge is slightly higher than on the first and central planes. With the more layers, asymmetric charge distribution disappears (Table 3). Lower value of effective atomic charge on the surface also indicates a significant covalent contribution to the chemical bonding of surface ions.

Table 2. Surface energy E_s (J/m²) for $(1\bar{1}00)$ and $(11\bar{2}0)$ surfaces of ZnO

Number of layers	PBE0		Number of layers	B3LYP [10]	
	$(1\bar{1}00)$	$(11\bar{2}0)$		$(10\bar{1}0)$	$(11\bar{2}0)$
5	2.27	1.37	8	1.4	1.4
7	2.26	1.37	10	1.4	1.4
9	2.26	1.37	12	1.3	1.4
11	2.26	1.37	14	1.3	1.4

Table 3. Effective charges $q_{eff}(e)$ of Zn and O atoms on $(1\bar{1}00)$ and $(11\bar{2}0)$ surfaces of ZnO

$(1\bar{1}00)$	Number of layers			
	5	7	9	11
Surface Zn	0.9	0.9	0.9	0.9
Subsurface Zn	0.93	0.92	0.92	0.92
Zn in central layer	0.91	0.97	0.97	0.97
Surface O	-0.83	-0.82	-0.82	-0.82
Subsurface O	-0.98	-0.96	-0.96	-0.96
O in central layer	-0.95	-0.96	-0.96	-0.96
$(11\bar{2}0)$				
Surface Zn	0.89	0.9	0.9	0.9
Subsurface Zn	0.95	0.95	0.95	0.95
Zn in central layer	0.95	0.96	0.96	0.96
Surface O	-0.86	-0.86	-0.86	-0.85
Subsurface O	-0.98	-0.98	-0.98	-0.98
O in central layer	-0.96	-0.96	-0.96	-0.96

Calculated vertical ionic displacements in the first and second atomic planes are given in Table 4. Both surfaces display significantly higher ionic relaxation in the first layer compared to the relaxation in the second layer. Displacement directions for Zn and O ions in the layers is controversial, Zn and O ions in the first layer are displaced inwards, whereas in the second layer they are displaced outwards. With more layers, relaxation slightly subsides; however, ionic relaxation for $(11\bar{2}0)$ surface is lower than for $(1\bar{1}00)$ surface for both layers. This result is in line with the surface energy calculation analysis (Table 2). Calculated ionic displacements $d(\text{Zn}) = -0.32$ Å and $d(\text{O}) = -0.1$ Å for $(1\bar{1}00)$ indicate the same relaxation picture as nonpolar $(10\bar{1}0)$ surface: O ions are higher than Zn ions [28, 29, 30].

Table 4. Vertical displacement Δz (Å) of Zn and O atoms on $(1\bar{1}00)$ and $(11\bar{2}0)$ ZnO surfaces depending on the number of layers in the slab. « \leftarrow » sign indicates displacement inward the slab.

Number of layers	$(1\bar{1}00)$				$(11\bar{2}0)$			
	Layer 1		Layer 2		Layer 1		Layer 2	
	Zn	O	Zn	O	Zn	O	Zn	O
5	-0.29	-0.09	+0.08	+0.03	-0.23	-0.08	+0.02	-0.01
7	-0.32	-0.11	+0.08	+0.02	-0.22	-0.08	+0.02	-0.02
9	-0.33	-0.11	+0.07	-0.01	-0.22	-0.07	+0.01	-0.02
11	-0.32	-0.11	+0.07	-0.01	-0.22	-0.07	+0.01	-0.02

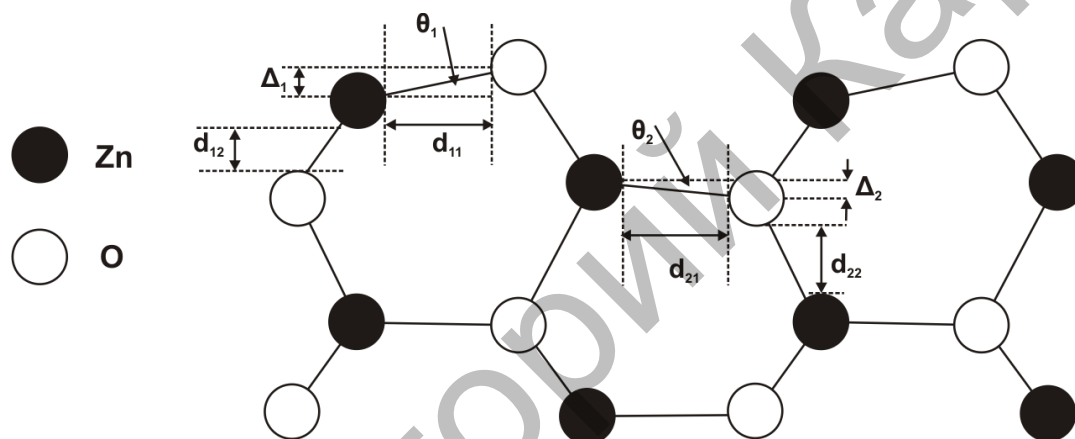
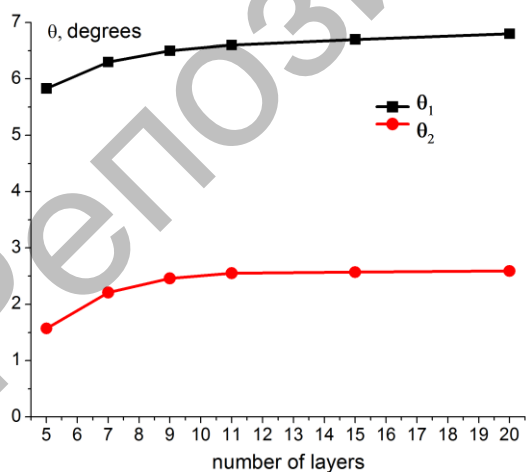
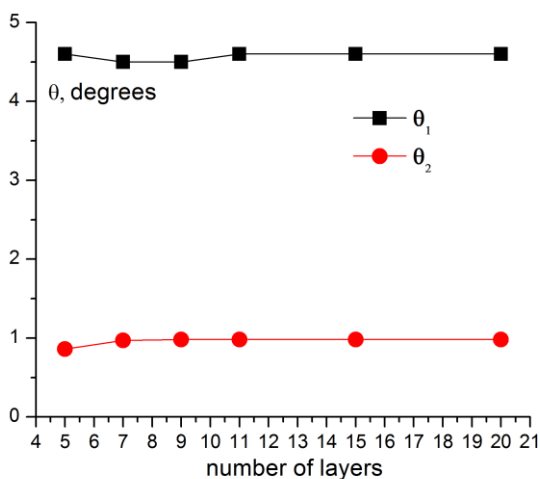


Fig.2. Side view of $(1\bar{1}00)$ surface and geometry relaxation parameters on the first and second atomic planes.

For $(11\bar{2}0)$ surface we have been used the same schematic representation.



a)



b)

Fig.3. Angular relaxation of Zn-O bond in the first and second surface layers depending on the number of layers in the surface slab (see Fig. 2): a) $(1\bar{1}00)$ surface b) $(11\bar{2}0)$ surface.

Angular relaxation of subsurface Zn-O bond is much smaller than for Zn-O bond on the first layer for both nonpolar surfaces (Fig. 3), but it still rather different from the bulk structure. For 20-layer atomic slab with $(1\bar{1}00)$ surface: $\theta_1 = 6.8^\circ$ and $\theta_2 = 2.6^\circ$, for the same slab with $(11\bar{2}0)$ surface: $\theta_1 = 4.6^\circ$ and $\theta_2 = 0.98^\circ$.

Table 5. Interlayer distances d_{12} and d_{22} (Å) on the first and second layers as presented in Fig. 2

Number of layers	$(10\bar{1}0)$		$(11\bar{2}0)$	
	Layer 1	Layer 2	Layer 1	Layer 2
5	0.620	1.9	1.405	1.617
7	0.616	1.932	1.421	1.637
9	0.618	1.936	1.426	1.652
11	0.628	1.937	1.429	1.640

Ionic relaxation also results in changed distance between atomic planes (Table 5). With the increase of number of layers, the interlayer distance gradually increases, both for $(1\bar{1}00)$ and $(11\bar{2}0)$ surface.

4. Conclusions

In this paper we have been performed *ab initio* hybrid calculations combined with PBE0 density functional and as results, we have been obtained the structural and electronic properties of nonpolar $(1\bar{1}00)$ and $(11\bar{2}0)$ ZnO surfaces. Full atomic and electronic relaxation results in the changed geometric arrangement of ions on the surfaces. In terms of surface energy, the $(11\bar{2}0)$ surface is more stable than $(1\bar{1}00)$ surface. Instability of $(1\bar{1}00)$ surface is also confirmed by the analysis of effective ionic charge distribution on the first and second layers.

The analysis of the absolute displacements of surface ions shows that after slab relaxation the surface Zn ions are displaced inwards, to the slab center, whereas O ions are shifted outwards, which is typical for metal oxide surfaces. This leads to a relatively small *surface rumpling*.

Calculations of angular relaxation as well as interlayer distances showed that ionic tilts reduce toward to the ZnO slab center, whereas interlayer distances are increase. This is lies in accordance with aforementioned tendency.

REFERENCES

1. D. C. Reynolds, D. C. Look, B. Jogai, C. W. Litton, G. Cantwell and W. C. Harsch Phys. Rev. B 60 2340 (1999)
2. C. R. A. Catlow, S. A. French, A. A. Sokol, A. A. Al-Sunadi and S. M. Woodley J. Comp. Chem. 29 2234 (2008)
3. P. D. C. King and T. D. Veal J. Phys.: Cond. Matt. 23 334214(2011)
4. M. D. McCluskey and S. J. Jokela J. Appl. Phys. 106 071101 (2009)
5. M. J. S. Spencer Progr. Mater. Sci. 57 437 (2012)
6. Q. Zhang, C. S. Dandeneau, X. Zhou and G. Cao Adv. Mater. 21 4087 (2009)
7. B. Meyer and D. Marx Phys. Rev. B 67 035403 (2003)
8. J.B. Hansen, Handbook of Heterogeneous Catalysis, G. Ertl, H. Knotzinger, J. Weitkamp (Eds.), Wiley-VCH, Weinheim, (1997)
9. C. G. Van de Walle and J. Neugebauer Nature 423 626 (2003)

10. N. L. V. Marana, M. Longo, E. Longo, J. B. L. Martins and J. R. J. Sambrano J. Phys. Chem. A 112 8958 (2008)
11. C. B. Duke, R. J. Meyer, A. Paton, and P. Mark Phys. Rev. B 18, 4225 (1978)
12. W. Gopel, J. Pollmann, I. Ivanov, and B. Reihl Phys. Rev. B 26, 3144 (1982).
13. A. Wander and N.M Harrison Surf. Sci. 457, L342 (2000).
14. A. Filippetti, V. Fiorentini, G. Cappellini, and A. Bosin Phys. Rev. B 59, 8026 (1999).
15. S. H. Na and C. H. Park Journal of the Korean Physical Society 54, №2, 867 (2009)
16. U. Diebold, L.V. Koplitz, O. Dulub App. Surf. Sc. 237, 336 (2004)
17. Y.R. Wang and C.B. Duke Surf. Sci. 192, 309 (1987)
18. I. Ivanov and J. Pollmann Phys. Rev. B 24, 7275 (1981)
19. Matz R and Lüth H Appl. Phys. 18, 123 (1979)
20. J P Perdew, M Ernzerhof, and K Burke J. Chem. Phys. 105, 9982 (1996)
21. R Dovesi, V R Saunders, R Roetti, R Orlando, C M Zicovich-Wilson, F Pascale, B Civalleri, K Doll, N M Harrison, I J Bush, P. D'Arco and M. Llunell 2009 CRYSTAL09 User's Manual University of Torino, Torino. URL: <http://www.crystal.unito.it>
22. J E Jaffe, A C Hess Phys. Rev. B 48 11 7903 – 7909 (1993)
23. C Gatti, V R Saunders, C Roetti. J Chem. Phys. 101 10686-10696 (1994)
24. M. J. D. Powell Numerical Methods for Non Linear Algebraic Equations; Gordon and Breach: London (1970)
25. F. Oba, A. Togo, I. Tanaka, J. Paier and G. Kresse Phys. Rev. B 77, 245202 (2008)
26. F. Gallino, G. Pacchioni and C. Valentin J. Chem. Phys. 133, 144512 (2010)
27. J. Albertsson, S. C. Abrahams, A. Kvik, Acta Crystallogr B45, 34 – 40 (1989)
28. N. Jedrecy, S. Gallini, M. Sauvage-Simkin, and R. Pinchaux Surf. Sci. 460, 136 (2000)
29. L. Whitmore, A.A. Sokol, and C.R.A. Catlow Surf. Sci. 498, 135 (2002)
30. P. Schroer, P. Kruger, and J. Pollmann Phys. Rev. B 49, 17092 (1994)